INTERNATIONAL JOURNAL OF OPTIMIZATION IN CIVIL ENGINEERING
Int. J. Optim. Civil Eng., 2023; 13(2):189-205

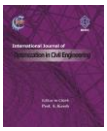

OPTIMAL PLACEMENT OF MAGNETO-RHEOLOGICAL DAMPERS USING NSGA-II-BASED FUZZY CONTROL

M. Payandeh-Sani and B. Ahmadi-Nedushan[*, †]
Department of Civil Engineering, Yazd University, Yazd, Iran.

[DOI: 10.22068/ijoce.2023.13.2.549]

ABSTRACT

In this study, the response of semi-actively controlled structures is investigated, with a focus on the effects of magneto-rheological (MR) damper distribution on the seismic response of structures such as drift and acceleration. The proposed model is closed loop, and the structure's response is used to determine the optimal MR damper voltage. A Fuzzy logic controller (FLC) is employed to calculate the optimum voltage of MR dampers. Drifts and velocities of the structure's stories are used as FLC inputs. The FLC parameters and the distribution of MR dampers across stories are determined using the NSGA-II, when the structure is subjected to the El-Centro earthquake, so as to minimize the peak inter-story drift ratio and peak acceleration simultaneously. The efficiency of the proposed approach is illustrated through a twenty-story nonlinear benchmark structure. Non-dominated solutions are obtained to minimize the inter-story drift and acceleration of structures and Pareto front produced. Then, the non-dominated solutions are used to control the seismic response of the benchmark structure, which was subjected to the Northridge, Kobe, and Hachinohe earthquake records. In the numerical example the maximum drift and acceleration decrease by about 36.3% and 15%, respectively, in the El-Centro earthquake. The results also demonstrate that the proposed controller is more efficient in reducing drift than reducing acceleration.

Keywords: Fuzzy logic controller, NSGA-II, multi-objective optimization, semi-active control, MR damper.

Received: 6 November 2022; Accepted: 7 January 2023

1. INTRODUCTION

In recent decades, various methods have been proposed to control structures against earthquakes [1, 2]. The structural control solutions proposed so far fall into four categories:

[*] Department of Civil Engineering, Yazd University, Yazd, Iran.
[†]E-mail address: behrooz.ahmadi@yazd.ac.ir (B. Ahmadi-Nedushan)

passive control [3], semi-active control [4], active control [5] and hybrid control [6]. MR dampers have been extensively studied as semi-active control instruments for civil engineering structures, due to their low energy requirements, simple mechanical structure, and suitable dynamic characteristics [7]. In MR dampers, electric energy is turned into mechanical energy in a controlled method to produce the damping force the structure needs [7]. Oliveira et al. [8] performed an experimental test in which they simulated the effect of earthquake acceleration on a model of a ten-story structure. They employed a semi-active control strategy that relied on MR dampers to mitigate the structural vibration caused by the earthquake. Their experimental results demonstrated the efficacy of proposed control system in reducing drift and absolute acceleration of considered structure. Liu et al. [9] compared the performance of various vibration control methods for a scaled bridge. MR fluid dampers were used in the bridge, controlled using energy optimization, Lyapunov, and the fuzzy logic control methods. When MR dampers are used in a structure, appropriate algorithms are always required to provide the desired voltage. Numerous control algorithms have been proposed and evaluated by researchers up to this point. These algorithms can be classified into two broad categories. In the first group of algorithms, a mathematical model is required to determine the suitable voltage for MR dampers [10-12]. The second category encompasses soft computing methods such as neural networks [5], fuzzy logic[13, 14], and neuro-fuzzy logic [15, 16]. The ability of smart control systems, such as fuzzy systems, to deal with nonlinear phenomena has increased their use[15]. Choi et al. [14] proposed a fuzzy semi-active control mechanism for reducing seismic response via a MR damper. Their proposed controller was designed to generate the required voltage directly from fuzzy rule-based system. This allowed the actuator to produce forces as close to the required forces as possible. Dounis et al. [17] applied evolutionary fuzzy logic control to design several structures subjected to seismic forces to minimize the base motion. Genetic algorithm was used to adjust the fuzzy logic parameters. Shariatmadar et al. [13] used the first and second type of fuzzy controller to calculate the appropriate voltage for the tuned mass utilized in the eleven-story benchmark building. Paul et al. [18] controlled a two-story structure using PD/PID and a Type 2 fuzzy logic system. It is well known that utilizing control instruments and algorithms can mitigate structural responses and structural damage in a structure. The decrease in the damage index of structures is directly proportional to the drift of its stories [19]. Thus, the damage can be considerably reduced in the structure by controlling the drift. In this article, We aim to find the optimal locations of MR-dampers using a meta-heuristic algorithm. Single and multi-objective meta-heuristic algorithms have been widely utilized in various fields of structural engineering such as structural optimization [20-22], structural damage detection [23, 24], structural reliability analysis [25], etc. In structural control, single and multi-objective optimization algorithms have been proposed in recent years. The single objective algorithm such as genetic algorithm [26], the particle swarm optimization algorithm [27], the hybrid PSO–GA algorithm [28], chaotic optimization algorithm [29] have all been successfully applied in the field of structural control. The process of optimizing systematically and simultaneously a collection of objective functions is called multi-objective optimization [30]. Most of the engineering and scientific applications have a multi-objective nature and require to optimize several conflicting objectives [31]. In contrast with single objective problems, the solution of multi-objective optimization algorithm is more of a concept than a definition. Typically, there is no single solution and solutions are

[DOI: 10.22068/ijoce.2023.13.2.549]

provided by a pareto front [32, 33]. Uz and Hadi [34] integrated multi-objective genetic algorithms and fuzzy logic to determine the distribution of MR dampers that operate as connective linkers between adjacent structures. Kwok et al. [35] utilized a multi-objective genetic algorithm to simultaneously minimize the number of MR dampers and resultant vibration magnitude. This article deals with a bi-objective optimization algorithm. The idea of simultaneous mitigation of drift and acceleration is used to minimize damage to the structure and equipment therein caused by the earthquakes. The semi-active control method and MR dampers are used to mitigate the seismic responses of structure. The FLC determines the optimal voltage of MR damper. The NSGA-II algorithm is used to determine the fuzzy system parameters and the optimal location of MR dampers. To demonstrate the efficiency of proposed methodology, a twenty-story benchmark structure was considered and exposed to the El-Centro earthquake records. Non-dominated solutions are obtained to minimize the inter-story drift and acceleration of structures and Pareto front is produced. Then, the non-dominated solutions are used to control the seismic response of the benchmark structure, which was subjected to the Northridge, Kobe, and Hachinohe earthquake records. Using the Pareto front, a designer can develop an appropriate view of MR dampers placement in the structure based on the structure's sensitivity to acceleration or drift.

The remainder of this article is structured as follows. The second section addresses the dynamic model of MR damper and the seismic properties of the benchmark structure. The NSGA-II is described in Section 3. The fourth section briefly describes fuzzy rule-based system. The fifth section describes the design of fuzzy controllers using NSGA-II and covers the results of a twenty-story benchmark structure. The conclusions constitute the final section.

2. MR DAMPER AND STRUCTURE MODELING

2.1 Three classical benchmarked functions

The dynamic behavior of MR damper is modeled using the well-known Bouc–Wen hysteresis model (Fig.1).

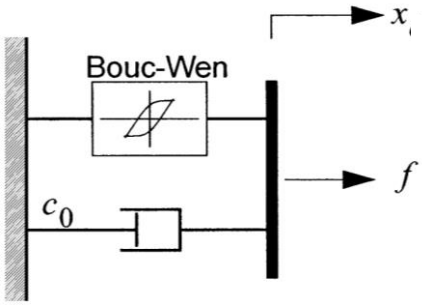

Figure 1. Mechanical model of MR damper [36]

The following equations are used to determine the force produced by MR damper:

[DOI: 10.22068/ijoce.2023.13.2.549]

$$f = c_0\dot{x} + \alpha z \tag{1}$$

$$\dot{z} = -\gamma|\dot{x}|z|z|^{n-1} - \beta\dot{x}|z|^n + A\dot{x} \tag{2}$$

$$\alpha = \alpha_a + \alpha_b u \tag{3}$$

$$c_0 = c_{0a} + c_{0b} u \tag{4}$$

In Eq. (1), $\dot{x}$ and c_0 denote MR damper's velocity and viscous damping, respectively, and z is the evolutionary variable. The first-order differential equation in Eq. (2) describes MR damper's hysteresis behavior. The variables η, γ, β, and A are shape parameters for the hysteresis loops of the yielding element in MR damper. The values of these parameters are presented in Table 1 [37].

Table 1: MR damper parameter [37]

Parameter	Value	Parameter	Value
$\alpha_a = 1.0872e2\ \frac{N}{cm}$	$\eta = 50s^{-1}$	$C_{0a} = 4.40\frac{N.s}{cm}$	$C_{\cdot b} = 44.0\frac{N.s}{cm.V}$
$\alpha_b = 4.9616e5\ \frac{N}{cm.V}$	$\gamma = 3\ cm^{-1}$	$A = 1.2$	$\beta = 3\ cm^{-1}$

2.2 Structural modeling

The nonlinear twenty-story benchmark structure shown in Fig. 2, is controlled by the proposed control method. The seismic mass of the first story is 5.63×10^5 Kg, the second to 19th story is 5.52×10^5 Kg, and the roof is 5.84×10^5 Kg. The lateral load-resisting of structure is moment-resisting frames. Interested readers are referred to the original article for complete details of this benchmark structure [38].

3. NSGA-II OPTIMIZATION ALGORITHM

The NSGA-II is one of the most widely used multi-objective optimization algorithms. It is distinguished by three unique qualities: a fast non-dominated sorting technique, a fast crowded distance estimation procedure, and a simple crowded comparison operator [39]. The flowchart of NSGA-II is depicted in Fig. 3.

In this study, the population size of NSGA-II is set as 220. The maximum number of

[DOI: 10.22068/ijoce.2023.13.2.549]

iterations is 100. These values were determined through trial and error.

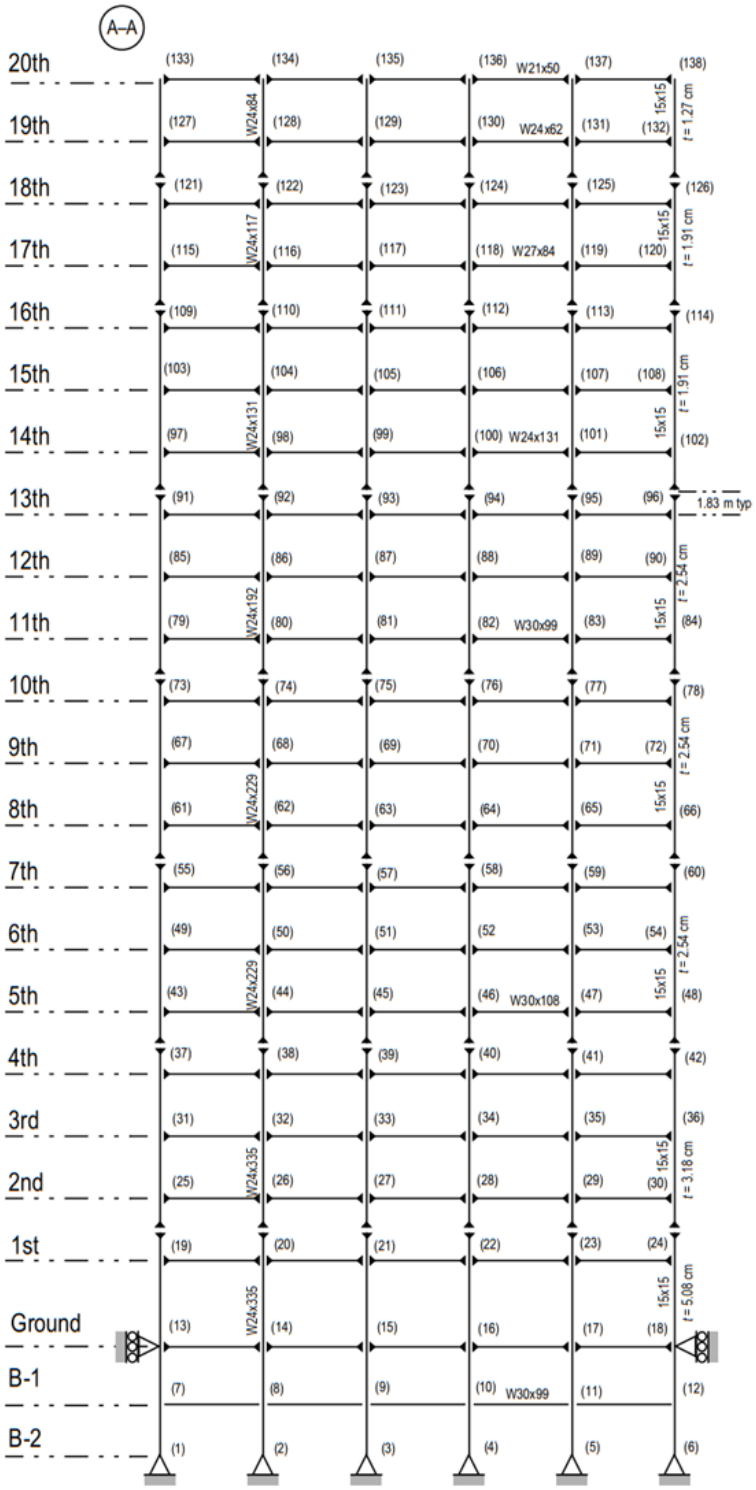

Figure 2. Twenty-story benchmark building north–south moment-resisting frame [38]

[DOI: 10.22068/ijoce.2023.13.2.549]

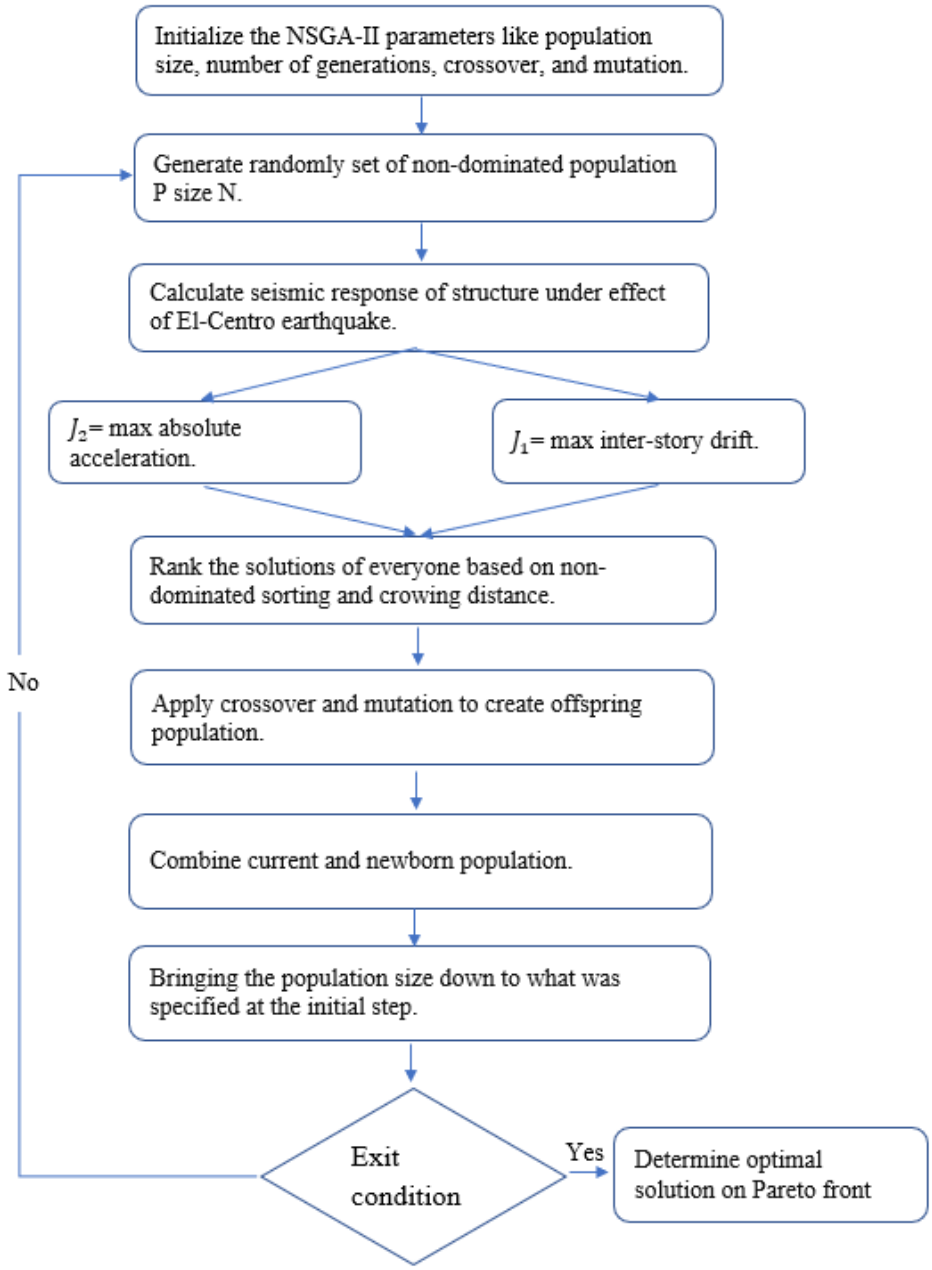

Figure 3. Flowchart for optimal design of FLC system based on NSGA-II

4. FLC ALGORITHM

The basic technique by which a FLC models the output from inputs is based on a series of if–then expressions known as fuzzy rules [40]. In this research, the inter-story drift ratio and relative velocity of MR dampers are chosen as the two input variables of the FLC, and the command voltage supplied to MR damper is the output variable. Fuzzy logic system

[DOI: 10.22068/ijoce.2023.13.2.549]

architecture is illustrated in Fig. 4. The interpretation of an if–then rule consists of two independent steps. The first step is to evaluate the antecedent, which entails fuzzifying the inputs and applying any fuzzy operators that are required, and the second step is to apply that result to the consequent.

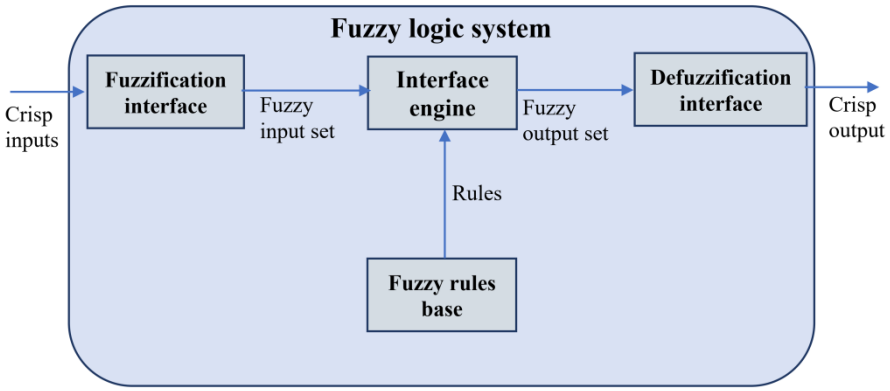

Figure 4. Fuzzy logic system architecture

One of primary units of a fuzzy logic control system is its rule base, which is a collection of if-then rules. Using a fuzzy reasoning mechanism, fuzzification unit converts the inputs, which may be in the form of crisp values, into fuzzy linguistic values. The fuzzy reasoning mechanism is the inference mechanism unit. This unit infers the control action for a fuzzy input using a variety of fuzzy logic procedures. Defuzzification is the transformation of fuzzy outputs into crisp outputs.

To design a FLC, in the first step, the FLC global structure must be determined. This step involves determining inputs and outputs, the number and type of membership functions (MF) for each input and output, as well as the type of inference mechanism, operators, and defuzzification method. In the subsequent step, FLC parameters are determined. In this step, MF parameters, the range of each input or output, and fuzzy rules are specified. MF parameters of FLC influence the structural response; therefore, determining these parameters is essential. In this article, Gaussian and sigmoidal MFs are used for defining the fuzzy sets for inputs and output (Fig. 5). The Gaussian and sigmoid MFs are defined by the fallowing equations:

The Gaussian membership function:

$$f(x;\sigma,c) = e^{\frac{-(x-c)}{2\sigma^2}} \tag{5}$$

The sigmoid membership function:

$$f(x;a,b)\frac{1}{1+e^{-a(x-b)}} \tag{6}$$

[DOI: 10.22068/ijoce.2023.13.2.549]

where σ and c, are the standard deviation and mean of Gaussian distribution. Parameters of sigmoid membership function, b and a, are the inflection point and the slope of the curve at the inflection point. When *a* is positive, the curve increases from left to right. Conversely, when *a* is negative, the curve decreases from left to right. In fuzzy logic input and output, the first and last MFs are sigmoidal, and the middle-ones are Gaussian.

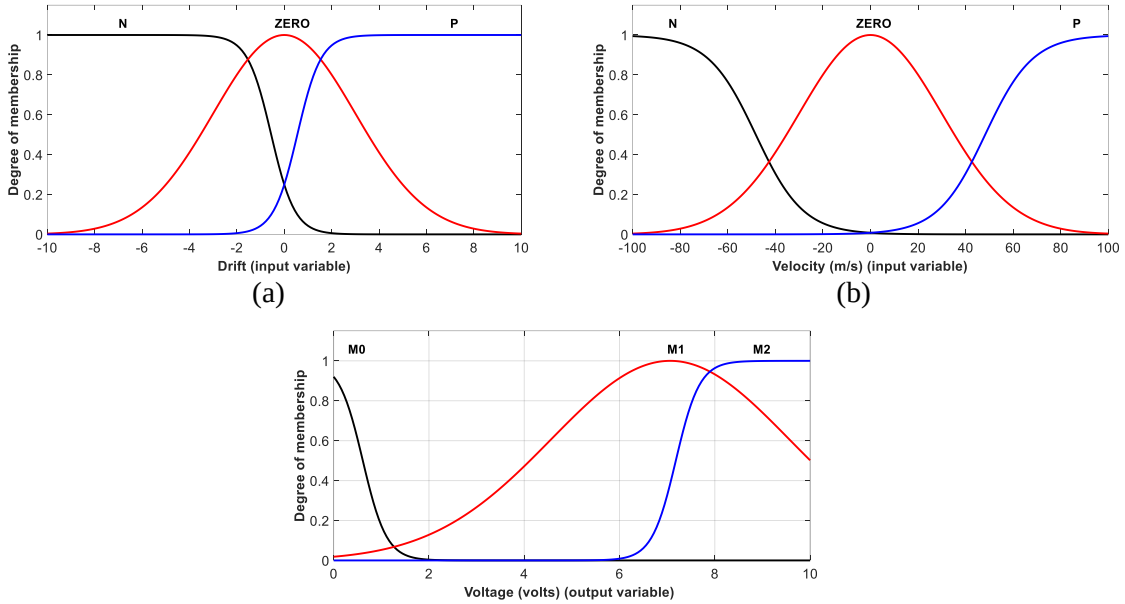

Figure 5. MFs for inputs and output: (a) drift, (b) velocity, and (c) drift

As shown in Table 2, fuzzy rules are designed using drift and velocity as the inputs and voltage as the output. In this Table, NV and PV, denote Negative and Positive velocity, respectively. Also, ND and PD, denote Negative and Positive drift, respectively. ZERO denotes the zero value of each input. The voltage range of MR dampers corresponds to the output range of FLC, which is 0-10 volts. The capacity of each MR damper is 1000 KN [41].

Table 2: The FLC rule base

	ND	ZERO	PD
NV	M2	M1	M0
ZERO	M1	M0	M1
PV	M0	M1	M2

5. DESIGN OF FUZZY CONTROLLER USING NSGA-II

The soft computing methods described in the preceding sections have been combined into a simple algorithm for solving the optimization problem of semi-active control of the structure while achieving the desired objectives. A FLC calculates the optimal voltage for MR

[DOI: 10.22068/ijoce.2023.13.2.549]

damper. The Bouc-wen model takes the relative velocity of the two ends of MR damper and the optimum voltage as inputs and applies the appropriate control force to the structure. Finding FLC parameters through trial and error is inefficient, and thus, optimization methods are used to determine the optimal value of FLC parameters that achieves the desired objectives. NSGA-II is employed to determine these parameters and the number of MR dampers installed on each story. After determining these parameters, the structure is controlled using the diagram depicted in Fig. 6.

The number of dampers in each floor and the fuzzy logic parameters constitute the optimization variables. There are twenty-five variables in total, in which twenty variables represent the number of dampers in each floor and five variables define the parameters of MFs.

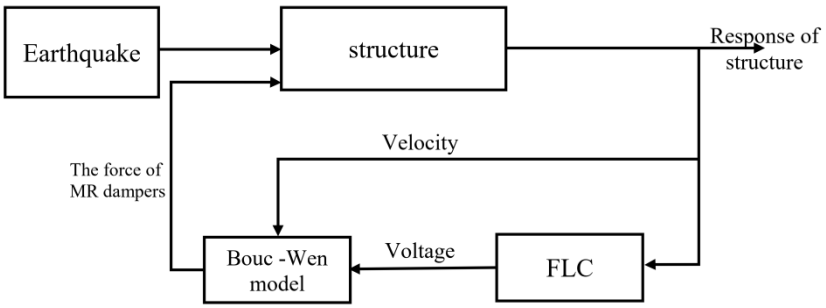

Figure 6. The structural control diagram

5.1 Dynamic analysis of the structure

The Newmark-β formulation is used to solve the differential equation of the structure's motion. These equations are solved at each time step. After calculating the structural responses at each step, the control force can be obtained at the next step. In 1959, Newmark proposed a class of time step formulations based on the following equations [42].

$$\dot{u}_{j+1} = \dot{u}_j + [(1-\gamma)\Delta t]\ddot{u}_j + (\gamma \Delta t)\ddot{u}_{j+1} \tag{7}$$

$$u_{j+1} = u_j + \Delta t\dot{u}_j + [(0.5-\beta)\Delta t^2]\ddot{u}_j + (\beta \Delta t^2)\ddot{u}_{j+1} \tag{8}$$

where $\ddot{u}_{j+1}$, u_{j+1}, and $\dot{u}_{j+1}$ are the acceleration, displacement, and velocity of the stories of the structure, respectively. Δt denotes the constant time steps. The factors γ and β denote the variations in acceleration at each time step, as well as the formulation's stability and accuracy. The values 1/2 and 1/6 are used for γ and β, respectively, assuming linear variations in the acceleration at each time step. U_{j+1}, $\dot{u}_{j+1}$ and $\ddot{u}_{j+1}$are calculated at time i+1 using equations (7) and (8) and the structure's motion equation at the end of the time step. Iterations are necessary to complete the analysis because $\ddot{u}_{j+1}$ is on the right-hand side of equations.

[DOI: 10.22068/ijoce.2023.13.2.549]

5.2 Evaluation criteria

In the numerical example which will be presented in the next section, the structure is controlled by different numbers of MR dampers. The following criteria are used to evaluate the performance of the proposed control mechanism [38].

$$J_1 = max\left\{\frac{max_{t.i}\left|{d_i(t)}/{h_i}\right|}{\delta_{max}}\right\} \tag{9}$$

$$J_2 = max\left\{\frac{max_{t.i}|\ddot{x}_{ai}(t)|}{\ddot{x}_{max}}\right\} \tag{10}$$

The criterion J_1 is related to the maximum inter-story drift. In equation (9), $\boldsymbol{d_i(t)}$ is the internal drift of the structure, h_i is the height of i-th story and $\boldsymbol{\delta_{max}}$ is its maximum value in the non-controlled state. The index J_2 is related to the maximum acceleration. The parameters $\boldsymbol{\ddot{x}_{ai}}$ and $\boldsymbol{\ddot{x}_{max}}$ are the i-th story acceleration in each time step in the controlled state and the maximum acceleration in the non-controlled state, respectively. Also, another criterion was defined to indirectly consider the cost associated with placing MR dampers in the structure. This index indicates the sum of the number of MR dampers in the structure.

$$J_3 = \sum_{i=1}^{20} n_i \tag{11}$$

In this equation, the number of MR dampers of i-th story is denoted by n_i. The number of MR dampers can be limited in the optimization algorithm to take the cost into account.

5.3 Numerical examples

Many numerical experiments were performed to evaluate the efficiency of proposed method. Based on the results obtained, the required changes were applied to the analysis to improve the performance of the proposed control mechanism. In this section, the proposed method is used to control the seismic response of the nonlinear benchmark twenty-story structure [38].

First, the FLC parameters and the number of MR dampers that must be placed in each story are determined using the NSGA-II algorithm. This is done to minimize the maximum acceleration and maximum inter-story drift, simultaneously. The optimization variables include the number of MR dampers in each story and the FLC parameters.

5.3.1 Determining optimal MR damper location

In the numerical example, the objective is to derive the Pareto front and to find the optimal location of MR dampers. The El-Centro earthquake record has been utilized to determine the FLC parameters. Fig. 7 shows the non-dominated solutions obtained from the NSGA-II algorithm. In this figure, the horizontal axis is the peak inter-story drift (J_1) of the

[DOI: 10.22068/ijoce.2023.13.2.549]

structure. The vertical axis (J_2) is the maximum acceleration of the structure.

The maximum number of MR dampers is limited to three dampers in each story. For the selected non-dominated solutions in Fig. 7 (S_1 and S_2), the number of MR dampers in each story and the evaluation criteria are presented in Table 3. The point with the lowest inter-story drift ratio is S1, while the point with the lowest peak acceleration is S2. If the objective of designer is to reduce the drift, the dampers can be placed according to point S1, and the associated fuzzy logic parameters are employed. If the equipment in the structure is sensitive to acceleration, point S2 can be selected as the design point and the dampers l and FLC parameters corresponding to this point are utilized.

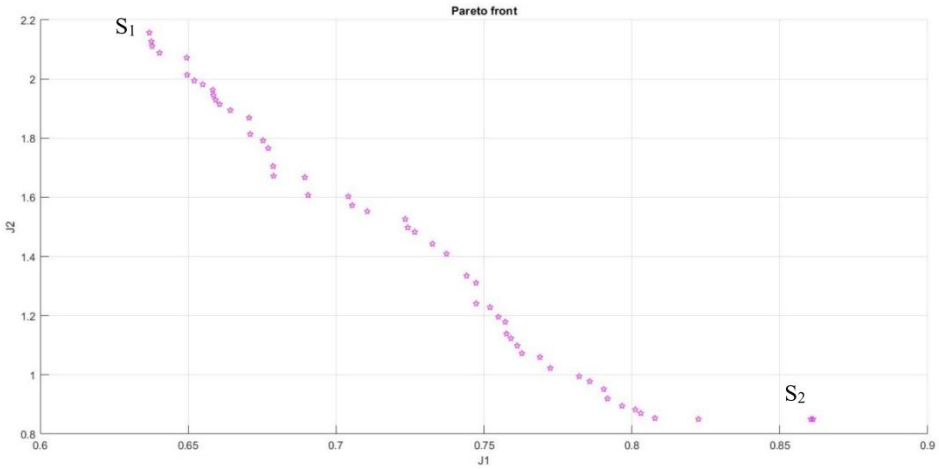

Figure 7. Non-dominated solutions obtained from the NSGA-II algorithm

Examining results presented in Table 3 reveals that the location of the dampers depends on the desired design objective. The fact that the number of dampers at points S_1 and S_2 is 28 and 21, respectively, indicates that if the design objective is to reduce the drift, a larger number of dampers are required. To compare arrangement of dampers for different objectives, the distribution of MR dampers at points S_1 and S_2 are also presented in Fig. 8.

Table 3: The FLC rule base

Story	S_1	S_2
1	3	1
2	3	2
3	3	1
4	3	2
5	0	1
6	0	0
7	1	0
8	1	0
9	0	0
10	1	2
11	0	0
12	0	2

[DOI: 10.22068/ijoce.2023.13.2.549]

13	0	1
14	3	3
15	2	0
16	1	3
17	2	2
18	0	0
19	3	1
20	2	0
J_1	0.6368	0.8612
J_2	2.1566	0.8496
J_3	28	21

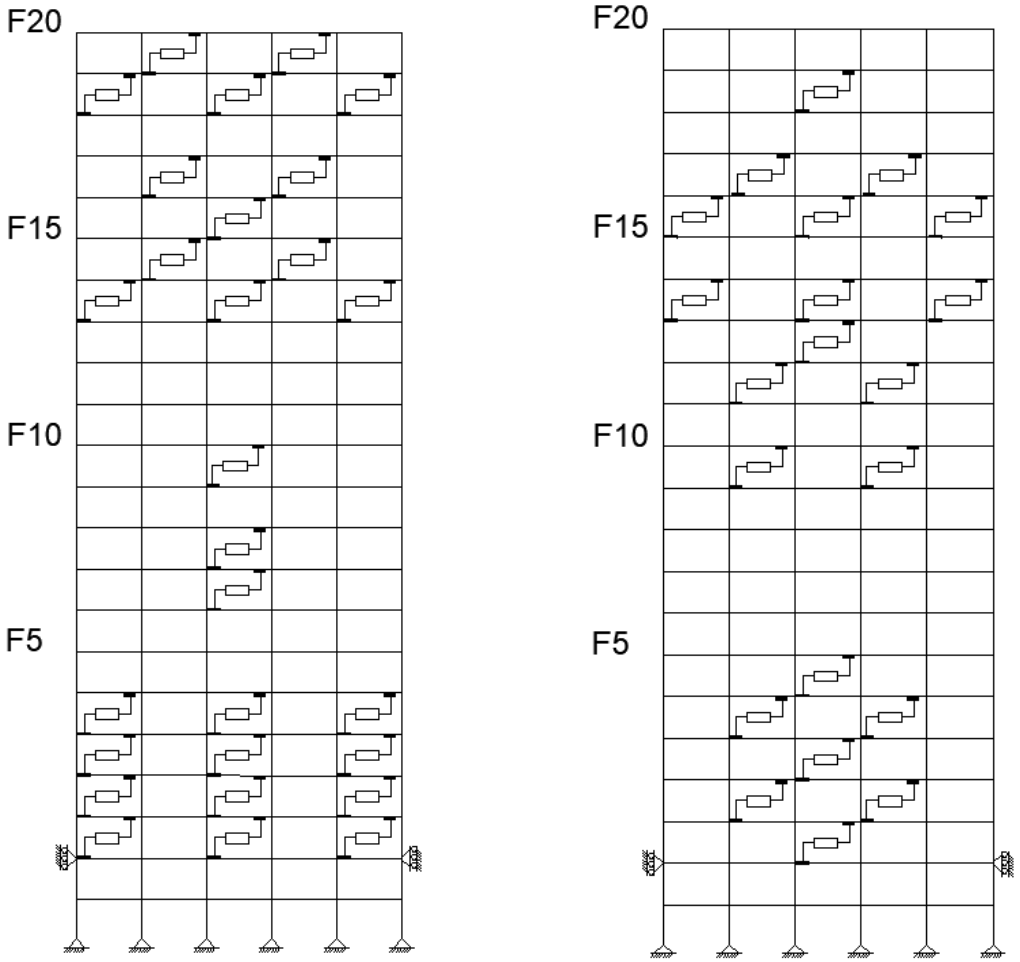

(a) (b)

Figure 8. Distribution of MR dampers in the first and last point of Pareto front: (a) Distribution of MR dampers in point S1, and (b) Distribution of MR dampers in point S2.

[DOI: 10.22068/ijoce.2023.13.2.549]

The Pareto front depicted in Fig. 7 can also be analyzed from a different viewpoint. The non-dominant solutions of Pareto front can be divided into two categories. The first category includes the designs which have a J_2 value of greater than one, whereas the designs of second category have a J_2 value of less than one. To study the distribution of dampers more precisely in accordance with the considered objective functions, the structural stories are divided into four groups of five, and the average number of dampers in each group is determined. Table 4 shows the average number of dampers in each group for two categories.

Table 4: The average number of dampers along the height of the structure

	Group 1	Group 2	Group 3	Group 4
Category 1	1.95	1.47	1.36	1.49
Category 2	1.89	1.23	1.56	1.38

The first group of floors consists of floors 1 to 5, the second group consists of floors 6 to 10, the third group consists of floors 11 to 15, and the fourth group consists of floors 16 to 20. As shown in the Table, when the purpose of structural control is to reduce drift, a larger number of dampers are required in lower stories. To evaluate the performance of the proposed method in other earthquakes, the solutions of Table 3 are used to control the benchmark structure under the effect of the Kobe, Northridge, and Hachinohe earthquakes records. The results are displayed in Table 5. It should be noted that the solutions obtained by the optimization algorithm are determined by analyzing the structure subjected to the El-Centro earthquake records and other records are not used in the optimization process. The results shown in Table 5 demonstrates that the maximum drift for the El-Centro, Northridge, Kobe, and Hachinohe earthquakes has been reduced by approximately 36.32%, 10%, 10% and 27.21%, respectively. The displacements of the first and the 20^{th} stories have been reduced about 2% and 10%, respectively, as depicted in Figs.9 and 10.

Table 5: Values of evaluation indices for El-Centro, Hachinohe, Kobe and Northridge earthquakes

Solution's number	El-Centro		Northridge		Kobe		Hachinohe	
	J_1	J_2	J_1	J_2	J_1	J_2	J_1	J_2
S1	0.6368	2.1566	0.9009	1.5632	0.9004	1.2207	0.7279	3.0981
S2	0.8612	0.8496	0.9773	0.9148	0.9120	0.8448	0.8740	1.0010

[DOI: 10.22068/ijoce.2023.13.2.549]

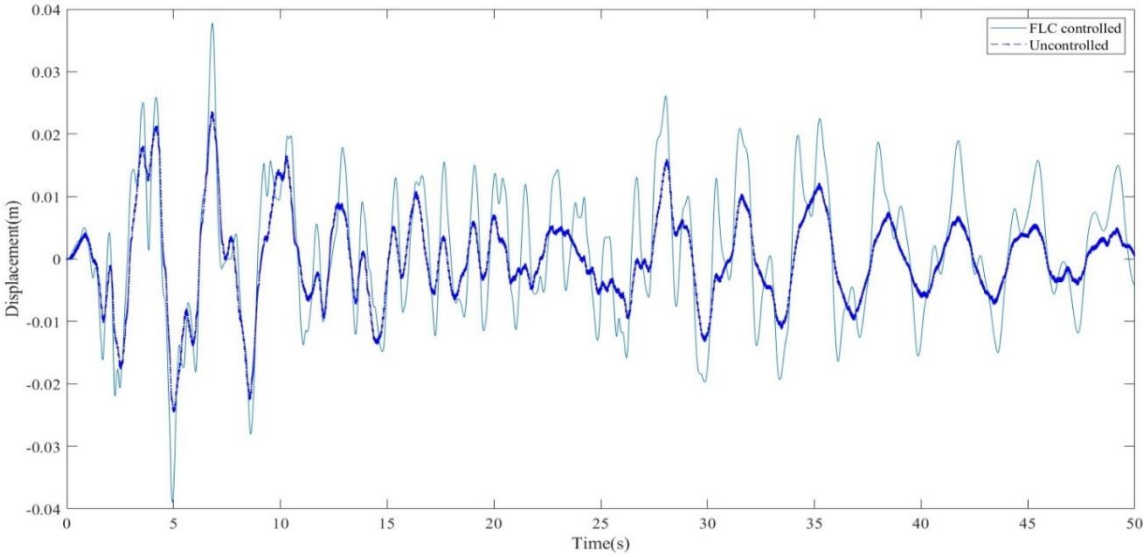

Figure 9. Displacement time histories of the first story subjected to El-Centro earthquake for uncontrolled and controlled structures

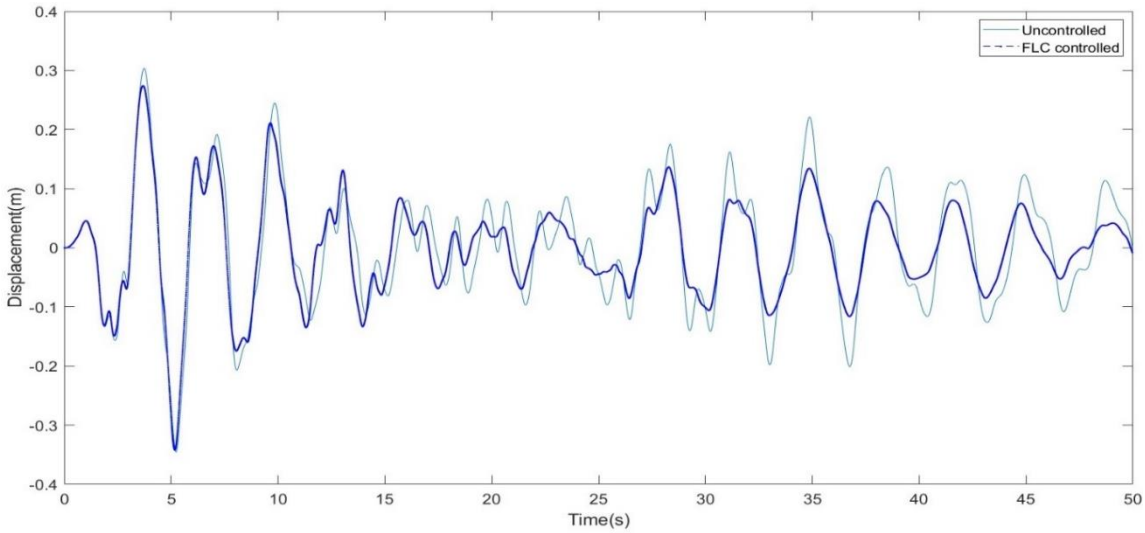

Figure 10. Displacement time histories of the 20th story subjected to El-Centro earthquake for uncontrolled and controlled structures

6. CONCLUSIONS

The purpose of this research is to find the optimal placement of MR dampers for the semi-active structural control. The FLC was used to control the nonlinear benchmark structure's seismic responses. The NSGA-II was utilized to find the best location of MR dampers and the optimal fuzzy logic parameters. To evaluate the efficiency of FLC, the El-Centro record was used. The NSGA-II provides various designs through Pareto fronts. The optimal

[DOI: 10.22068/ijoce.2023.13.2.549]

solution can be selected from points of Pareto fronts by considering the objective of structural control design. The presented results indicate that the optimal location and number of MR dampers is different when the design objective is reducing the drift or acceleration. Thus, the designer can find the best distribution of MR dampers according to the sensitivity of the structure to drift or the sensitivity of the equipment within the structure to acceleration. For earthquakes considered in this study, performance of proposed method in controlling structures subjected to far-field earthquakes is superior to that of near-field earthquakes, as the maximum inter-story drift during the El-Centro and Hachinohe earthquake decreased by 36.32% and 27.21%, respectively, while the reductions in the Northridge and Kobe earthquake are about 10% and 10%, respectively. It can be also concluded that the proposed control method is more effective in reducing structure drift than reducing acceleration. Comparing the number of dampers at various points along the Pareto front, it can be seen that a larger number of dampers are required when the objective is to reduce relative inter-story drift compared to the case where the objective is to reduce structure acceleration.

REFERENCES

1. Kaveh A, Pirgholizadeh S, Khadem Hosseini O. Semi-active tuned mass damper performance with optimized fuzzy controller using CSS algorithm, *Asian J Civ Eng*, 2015; **16**(5): 587-606.
2. Saaed TE, Nikolakopoulos G, Jonasson J-E, Hedlund H. A state-of-the-art review of structural control systems, *J Vib Control*, 2015; **21**(5): 919-37.
3. Kaveh A, Fahimi Farzam M, Hojat Jalali H, Maroofiazar R. Robust optimum design of a tuned mass damper inerter, *Acta Mech*, 2020; **231**(9): 3871-96.
4. Yanik A. Seismic control performance indices for magneto-rheological dampers considering simple soil-structure interaction, *Soil Dyn. Earthq. Eng.*, 2020; **129**: 105964.
5. Rezaiee-Pajand M, Payandeh Sani M. Three schemes for active control of the planer frame, *Int J Optim Civil Eng*, 2015; **5**(1): 117-35.
6. Soto MG, Adeli H, Semi-active vibration control of smart isolated highway bridge structures using replicator dynamics, *Eng Struct*, 2019; **186**: 536-552.
7. Spencer BF, Carlson JD, Sain MK, Yang G. *On the current status of magnetorheological dampers: seismic protection of full-scale structures*. in *Proceedings of the 1997 American Control Conference* 1997. New Mexico, USA.
8. Oliveira F, Botto MA, Morais P, Suleman A. Semi-active structural vibration control of base-isolated buildings using magnetorheological dampers, *J Low Freq Noise Vib Act Control*, 2018; **37**(3): 565-76.
9. Liu Y, Gordaninejad F. Evrensel CA, Wang X, Hitchcock G, Comparative study on vibration control of a scaled bridge using fail-safe magneto-rheological fluid dampers, *J Struct Eng*, 2005; **131**(5): 743-51.
10. Heidari AH, Etedali S, Javaheri-Tafti MR. A hybrid LQR-PID control design for seismic control of buildings equipped with ATMD, *Front Struct Civ Eng*, 2018; **12**(1): 44-57.

[DOI: 10.22068/ijoce.2023.13.2.549]

11. Kaveh A, Farzam MF, Maroofiazar R. Comparing H2 and H∞ algorithms for optimum design of tuned mass dampers under near-fault and far-fault earthquake motions, *Period Polytech Civ Eng*, 2020; **64**(3): 828-44.
12. Fallah AY, Taghikhany T, Robust semi-active control for uncertain structures and smart dampers, *Smart Mater Struct*, 2014; **23**(9): 095040.
13. Shariatmadar H, Golnargesi S, Akbarzadeh T. Vibration control of buildings using ATMD against earthquake excitations through interval type-2 fuzzy logic controller, *Asian J Civ Eng*, 2014; **15**: 321-38.
14. Choi KM, Cho SW, Jung HJ, Lee IW. Semi-active fuzzy control for seismic response reduction using magnetorheological dampers, *Earthq Eng Struct Dyn*, 2004; **33**(6): 723-36.
15. Gu X, Yu Y, Li Y, Li J, Askari M, Samali B. Experimental study of semi-active magnetorheological elastomer base isolation system using optimal neuro fuzzy logic control, *Mech Syst Signal*, 2019; **119**: 380-98.
16. Bozorgvar M, Zahrai SM. Semi-active seismic control of buildings using MR damper and adaptive neural-fuzzy intelligent controller optimized with genetic algorithm, *J Vib Control*, 2019; **25**(2): 273-85.
17. Dounis A, Tiropanis P, Syrcos G, Tseles D. Evolutionary fuzzy logic control of base-isolated structures in response to earthquake activity, *Structural Control and Health Monitoring: The Official Journal of the International Association for Structural Control and Monitoring and of the European Association for the Control of Structures*, 2007; **14**(1): 62-82.
18. Paul S, Yu W, Li X. Bidirectional active control of structures with type-2 fuzzy PD and PID, *Int J Syst Sci*, 2018; **49**(4): 766-82.
19. Kazemi MS, Behnamfar F. Active control of structures based on an arbitrary damage index distribution, *AUT J Civil Eng*, 2020; **4**(3): 385-396.
20. Kaveh A, Laknejadi K, Alinejad B. Performance-based multi-objective optimization of large steel structures, *Acta Mech*, 2012; **223**(2): 355-69.
21. Kaveh A, Zaerreza A. Shuffled shepherd optimization method: A new meta-heuristic algorithm, *Eng Comput*, 2020; 37(7): 2357-89,
22. Kaveh A, Gholipour Y, Rahami H, Optimal design of transmission towers using genetic algorithm and neural networks, *Int J Space Struct.*, 2008; **23**(1): 1-19.
23. Fathnejat H, Ahmadi-Nedushan B. An efficient two-stage approach for structural damage detection using meta-heuristic algorithms and group method of data handling surrogate model, *Front Struct Civ Eng*, 2020; **14**(4): 907-29.
24. Ahmadi-Nedushan B, Fathnejat H. A modified teaching–learning optimization algorithm for structural damage detection using a novel damage index based on modal flexibility and strain energy under environmental variations, *Eng Comput*, 2022: 1-32.
25. Seyyed Jafari M, Gholizadeh S. Reliability analysis of optimally designed double layer barrel vaults *Int J Optim Civil Eng*, 2021; **11**(3): 383-96.
26. Hashemi SMA, Haji Kazemi H, Karamodin A. Localized genetically optimized wavelet neural network for semi-active control of buildings subjected to earthquake, *Struct Control Health Monit*, 2016; **23**(8): 1074-87.
27. Zabihi Samani M, Ghanooni-Bagha M. A fuzzy logic controller for optimal structural control using MR dampers and particle swarm optimization, *J Vibroengineering*, 2017;

[DOI: 10.22068/ijoce.2023.13.2.549]

19(3): 1901-14.
28. Martínez-Soto R, Castillo O, Aguilar LT. Type-1 and Type-2 fuzzy logic controller design using a Hybrid PSO–GA optimization method, *Inf Sci*, 2014; **285**: 35-49.
29. Kaveh A, Javadi SM, Mahdipour Moghanni R. Optimal structural control of tall buildings using tuned mass dampers via chaotic optimization algorithm, *Structures*, 2020; **28**: 2704-13.
30. Marler RT, Arora JS. Survey of multi-objective optimization methods for engineering, *Struct Multidiscip Optim*, 2004; **26**(6): 369-95.
31. Kaveh A, Ilchi Ghazaan M. A new VPS-based algorithm for multi-objective optimization problems, *Eng Comput*, 2020; **36**(3): 1029-40.
32. Jahangiri M, Ahmadi-Nedushan B, Rahimi Bondarabadi H. *Structural damage localization and quantification based on multi-objective optimization method*. in *2nd International & 6th National Conference on Earthquake & Structures, At ACECR of Kerman, Kerman, Iran*. 2015.
33. Jahangiri M, Ahmadi-Nedushan B, Structural damage identification using MOPSO and MOEA/D multi-objective evolutionary optimization algorithms, *J Ferdowsi Civil Eng*, 2016; **30**(1): 63-77.
34. Uz ME, Hadi MNS, Optimal design of semi active control for adjacent buildings connected by MR damper based on integrated fuzzy logic and multi-objective genetic algorithm, *Eng Struct*, 2014; **69**: 135-48.
35. Kwok N, Ha Q, Samali B. *MR damper optimal placement for semi-active control of buildings using an efficient multi-objective binary genetic algorithm*. in *Automation and Robotics in Construction-Proceedings of the 24th International Symposium on Automation and Robotics in Construction*. 2007. India.
36. Jansen LM, Dyke SJ, Semiactive control strategies for MR dampers: comparative study, *J Eng Mech*, 2000; **126**(8): 795-803.
37. Khaje-Karamodin A, Rowhanimanesh A, Akbarzadeh-Tootoonchi M, Haji-Kazemi H. Semi-active control of structures using a neuro-inverse model of MR dampers, *Scientia Iranica*, 2009; **16**(3):
38. Ohtori Y, Christenson R, Spencer Jr B, Dyke S. Benchmark control problems for seismically excited nonlinear buildings, *J Eng Mech*, 2004; **130**(4): 366-85.
39. Deb K, Pratap A, Agarwal S, Meyarivan T. A fast and elitist multiobjective genetic algorithm: NSGA-II, *IEEE T Evol Comput*, 2002; **6**(2): 182-97.
40. Kim H-S, Kang J-W. Semi-active fuzzy control of a wind-excited tall building using multi-objective genetic algorithm, *Eng Struct*, 2012; **41**: 242-57.
41. Bitaraf M, Hurlebaus S. Semi-active adaptive control of seismically excited 20-story nonlinear building, *Eng Struct*, 2013; **56**: 2107-18.
42. Chopra KA. *Dynamic of Structures:Theory and Applications to Earthquake Engineering*. fourth ed. 2012: Prentice Hall.

[DOI: 10.22068/ijoce.2023.13.2.549]